

# Numerical research on unsteady cavitating flow over a hydrofoil

D Homa<sup>1,2</sup> and W Wróblewski<sup>1</sup>

<sup>1</sup>Institute of Power Engineering and Turbomachinery, Silesian University of Technology, Konarskiego Street 18, Gliwice, Poland

<sup>2</sup>To whom any correspondence should be addressed

**Abstract.** Cavitation is a widely known phenomenon in pumps and water turbines installations. It can lead to significant damage of blades and walls of the rotor therefore it is crucial during pump designing and exploitation to avoid working in flow conditions, that enabled cavitation to occur. Nowadays numerical simulations of flow can provide valuable information concerning pressure and velocity distribution and can indicate if there is a risk of cavitating flow appearance. There are a few mathematical models which describe cavitating flow. In the paper Schnerr & Sauer model was chosen for simulation. Aim of the paper is to verify its utility in case of different cavitating flow regimes over Clark-Y hydrofoil. After performing the grid independence study four different cavitation regimes were investigated. The vapour areas appearance, their shapes and changes in time were observed. The assumption of isothermal, two – phase flow was made. The calculations were performed using OpenFOAM and were compared to the available measurements data. The presented results concerned sheet and cloud cavitation regimes.

## 1. Introduction

Cavitation phenomenon was first observed and described by Osborne Reynolds in 1894. It is a complex process of forming and collapsing vapour bubbles in liquid flow. The formation and growth of bubbles is possible under low pressure conditions. The bubbles next flow into higher pressure region and collapse suddenly. It leads to great pressure and temperature augmentation at the bubble center. The pressure wave is generated and it propagates through the flow. It causes high frequency noise which is one of first cavitation symptoms. The others effects of cavitating flow occurrence are vibrations and erosion of solid surfaces near cavitation structures. The detailed descriptions of bubble physics and cavitation types can be found in work of Brennen [1] and Franc and Michel [2]. Numerical modelling of cavitating flow has to deal with instabilities on liquid – vapour interface, at which large variations in structures size and velocity over short periods appear. The scaling of cavitation phenomenon is challenging, taking into consideration that collapse of a single bubble takes about one millisecond, but collapse of a whole structure – order of microseconds. According to the [2], the velocities of an interface vary between meters per second to hundreds of meters per second. The gauge pressure generated by the implosion of cavitation structures can reach several thousand bars. Regarding to all these facts the numerical modelling of cavitation make use of some simplifications of the process, such as negligence of the surface tension.

The topic of following investigation was flow over a foil. For this type of flow, which is typical for pumps' rotors, the characteristic dimensionless variable is called cavitation number  $\sigma$ , which is defined as [1, 2]:



$$\sigma = \frac{p - p_s}{0.5 \rho_l u_\infty^2} \quad (1)$$

where:  $p$  – pressure, Pa;  $p_s$  – saturation pressure, Pa;  $\rho_l$  – liquid density,  $\text{kg}\cdot\text{m}^{-3}$ ;  $u_\infty$  - free stream velocity,  $\text{m}\cdot\text{s}^{-1}$ .

With decrease of cavitation number the following cavitation regimes can be observed: incipient, sheet, cloud and supercavitation [3]. Wang et al. [3] performed an experiment including flow over Clark-Y foil and provided wide range of information about cavitation dynamics and structures for these four cavitation regimes. The aim of the following study was to verify results obtained by means of Schnerr & Sauer model in case of two cavitation regimes: sheet and cloud cavitation. The sheet type cavitation is the first type when the developed cavitation structures can be observed. Sheet cavitation occurs when cavitation number  $\sigma$  reaches 1.4 [3]. According to [3] it is characterized by finger-like structure of vapour-water interface on the leading edge of the blade. Such shape is due to the combination of different vortex pairs and detachment of the head of each pair. However, the rear region of the sheet is unsteady and rolls up into a series of bubbly eddy that are shed intermittently. The frequency of changes of the whole structures is about 200 Hz (period 5 of ms). The next cavitation regime is called cloud cavitation. It occurs when cavitation number drops to 0.8 [3]. The frequency of cloud cavitation for these parameters is equal to 20 Hz (50 ms for one cycle). It is characteristic of attached front portion and unsteady rear region. In the beginning of the cycle, the cavity is attached near the leading edge. It grows and travels downstream with packet of bubbles moving with a clockwise rotation till about the midpoint of the cycle. Then the massive vortex shedding appears. Due to large-scale vortex dynamics the higher pressure near wall region occurs and cavitating flow is pushed away from the wall. A re-entrant flow in the wall region is induced toward the upstream. As it reaches the vicinity of leading edge of the cavity, the existing cavitating flow detaches from the wall and a new cavitating flow structure forms there.

## 2. Cavitation model

Cavitation modelling methods can be gathered into two main groups: one-fluid and two-fluid models [4]. In one-fluid models group the flow is assumed to be a mixture of two phases and the conservation equations (mass and momentum) for the mixture are to be solved. In this simulation no slip between the phases was assumed. To calculate fraction of gaseous phase mass conservation equation of vapour is solved [4]:

$$\frac{\partial \alpha \rho_v}{\partial t} + \nabla(\alpha \rho_v u) = \begin{cases} R_e & p \leq p_s \\ -R_c & p > p_s \end{cases} \quad (2)$$

where:  $\alpha$  – vapour volume fraction, -;  $\rho_v$  – vapour density,  $\text{kg}\cdot\text{m}^{-3}$ ;  $u$  – velocity,  $\text{m}\cdot\text{s}^{-1}$ ;  $R_e$ ,  $R_c$  – source terms,  $\text{kg}\cdot\text{m}^{-3}\cdot\text{s}^{-1}$ .

In Schnerr & Sauer model the source terms are derived from Rayleigh-Plesset (RP) equation, which describes the dynamics of vapour bubbles. The RP equation is simplified, no surface tension is assumed, as in formula below [1]:

$$\frac{Dr_B}{Dt} = \sqrt{\frac{2}{3} \frac{p_B - p}{\rho_l}} \quad (3)$$

where:  $r_B$  – radius of bubble, m;  $p_B$  – pressure in the bubble, Pa.

The final formulas for source terms are as follows [5]:

$$R_e = \frac{\rho_l \rho_v}{\rho} \alpha (1 - \alpha) \frac{3}{r_B} \sqrt{\frac{2}{3} \frac{p_s - p}{\rho_l}} \quad (4)$$

$$R_c = \frac{\rho_l \rho_v}{\rho} \alpha (1 - \alpha) \frac{3}{r_B} \sqrt{\frac{2}{3} \frac{p - p_s}{\rho_l}} \quad (5)$$

Where:  $\rho$  – mixture density, derived from volume fractions and densities of the phases,  $\text{kg}\cdot\text{m}^{-3}$ .

The radius of bubble  $r_B$  is derived from vapour volume fraction and number of bubbles per volume of liquid  $n_B$ , using the following relation [5]:

$$r_B = \left( \frac{\alpha}{1-\alpha} \frac{3}{4\pi} \frac{1}{n_B} \right)^{\frac{1}{3}} \quad (6)$$

Number of bubbles per volume of liquid is to be set as the model constant.

### 3. Numerical model description

#### 3.1. Geometry

The simulation concerned flow over a Clark-Y hydrofoil. It is a typical foil used in water machinery. The overview of the geometry is shown in figure 1.

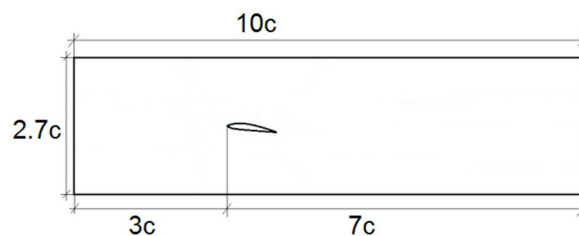


**Figure 1.** Overview of the geometry.

The foil was placed in distance of  $3c$  from the inlet and  $7c$  from the outlet, as the cavitation structures can reach much further than the chord length. The height of the channel was set to  $2.7c$  and foil was placed symmetrically from the upper and lower wall of the channel. Chord of the foil was equal to  $70 \text{ mm}$ .

#### 3.2. Grid parameters

The 3D grid was made by means of ICEM CFD software. The geometry has been divided into 8 blocks and the O-grid was generated around the blade. The blade profile was split into 4 edges: near leading edge, upper side, lower side and trailing edge. On lower and upper side edges 85 grid nodes were set, on the leading and trailing edges – 30 nodes. The surface block mesh was used at first, next it was extruded in the perpendicular direction by 10 layers of elements of  $1 \text{ mm}$  thickness each. The whole mesh consisted of 216k hexahedra elements. The overview of the mesh is shown in figure 2.

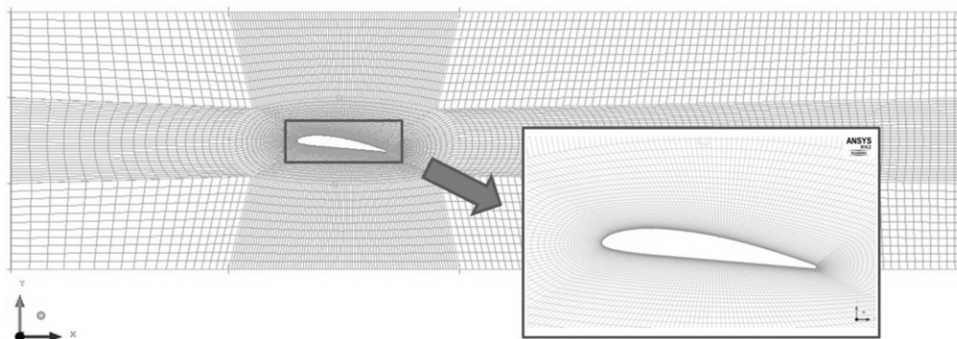


**Figure 2.** Overview of the mesh, zoom of the O-grid region.

#### 3.3. Calculations set up

The simulation was performed with assumption of constant inlet velocity. The pressure at the outlet

was consequently lowered. For sheet cavitation the outlet pressure was equal to 72 000 Pa, for cloud cavitation: 42 260 Pa. The calculations were performed in OpenFOAM open source code with the solver *interPhaseChangeFoam*, which captures well the dynamics of the cavitating flow [6]. The simulation set up was based on other investigations [7-9], the turbulence model was *k- $\omega$  SST*, chosen after literature study [10-12]. The adjustable time step was used, with the condition that Courant number must remain under 1. The transient, first order numerical scheme was chosen. The simulation set up is shown in table 1.

**Table 1.** Calculation set up (bc – boundary condition).

|                               |                                  |
|-------------------------------|----------------------------------|
| Chord length                  | 70 mm                            |
| Angle of attack               | 8°                               |
| Heat transfer model           | Isothermal                       |
| Flow temperature              | 20°C                             |
| Turbulence model              | <i>k-<math>\omega</math> SST</i> |
| Side walls bc                 | Symmetry                         |
| Upper/lower wall bc           | Wall                             |
| Outlet bc                     | Static pressure (case dependent) |
| Inlet velocity                | 10 m/s                           |
| Turbulence intensity at inlet | 5%                               |
| Reynolds number               | 700 000                          |
| $n_B$ in Schnerr&Sauer model  | $1.6 \times 10^{13}$ [5]         |
| $r_B$ in Schnerr&Sauer model  | $10^{-6}$ m [5]                  |

#### 4. Results

The end of the calculation was determined by the end time. The final residuals dropped to the level of  $10^{-6}$ . The maximum values of  $y^+$  on the foil were equal to 21.1 on the upper and lower side and 32.4 in the elements near leading and trailing edge.

##### 4.1. Structures description

The calculations were performed for two different cavitation regimes: sheet and cloud cavitation. In figure 3. one period of changes for each cavitation model is shown. For both regimes the periodic changes of structures growth and collapse were observed. The chosen parameters of changes are compared in table 2.

**Table 2.** Comparison of calculations results.

| Parameter   | Sheet cavitation           | Cloud cavitation    |
|---|----------------------------|---------------------|
| Shedding frequency  | 32 Hz                      | 30 Hz               |
| Period  | 31 ms                      | 33 ms               |
| Beginning of the structure coordinate (measured from beginning of the foil) | X=0.1038 mm<br>Y=0.1886 mm | X=3.31mm<br>Y=2.6mm |
| Maximum height of a structure   | 12 mm                      | 13 mm               |
| Maximum length of a structure   | 81 mm                      | 104 mm              |

The frequency of shedding for sheet cavitation is much lower compared to the available measurement data [3], which states that the frequency is equal to 200 Hz. For cloud cavitation the frequency is lower comparing to the sheet cavitation regime, which is compatible to the observations [3]. The frequency observed during calculations is similar to the one described in [3], equal to 30 Hz. For cloud cavitation regime the cavitation structures beginning was located further that for sheet cavitation regime, which is shown in figure 4. The maximum height and length of the cavitation structures grew as the cavitation number decreased. For both regimes they occurred after 2/3 of the period. The dynamics of cavitation structures was different for the two investigated flows. First the

bubble cluster was formed, starting from leading edge and covered whole of the upper side of the foil for sheet cavitation after  $5/12$  of the period, for cloud cavitation after  $1/3$  of the period.

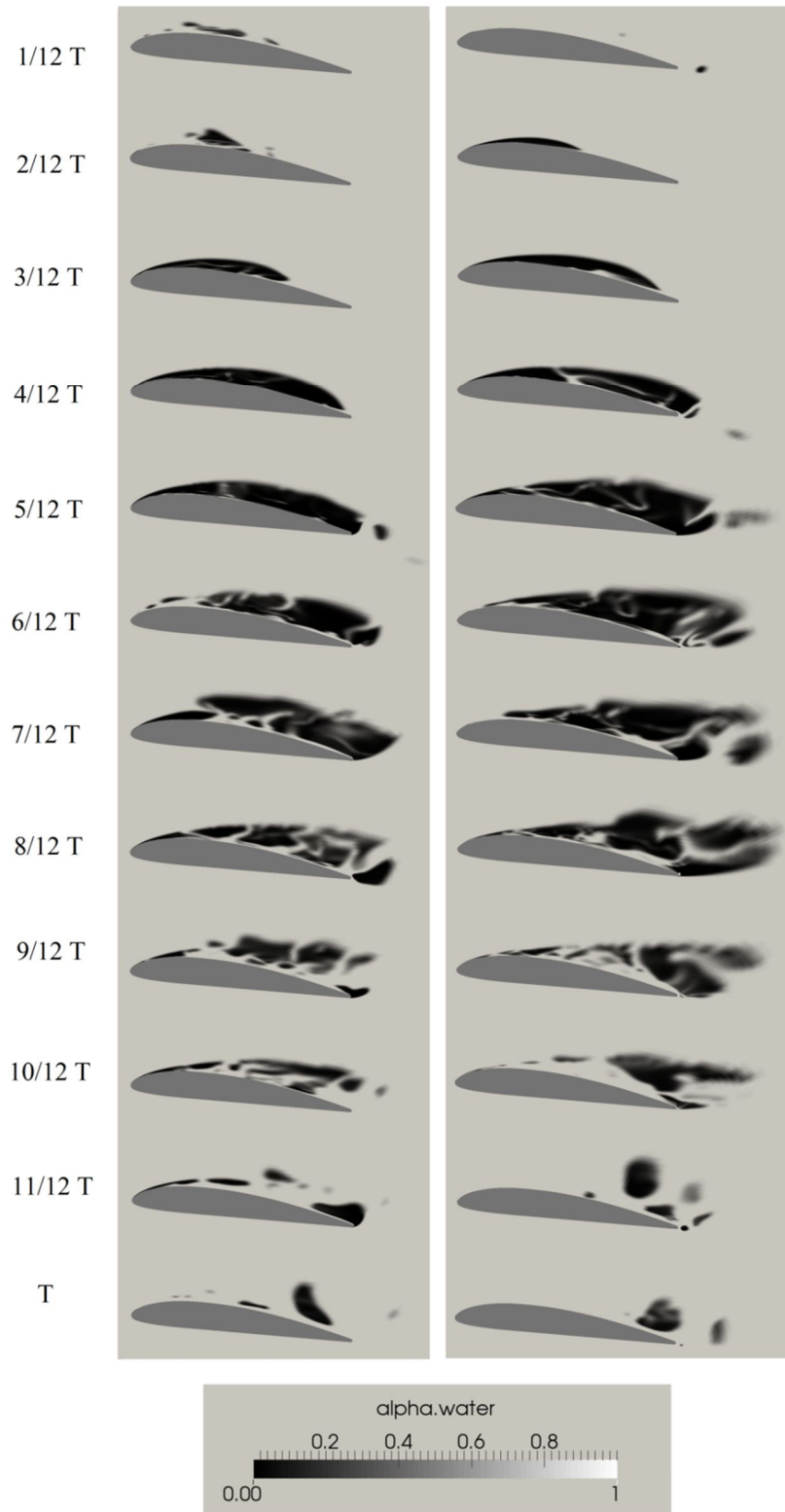


**Figure 3.** One period of changes for sheet cavitation – left, cloud cavitation – right.

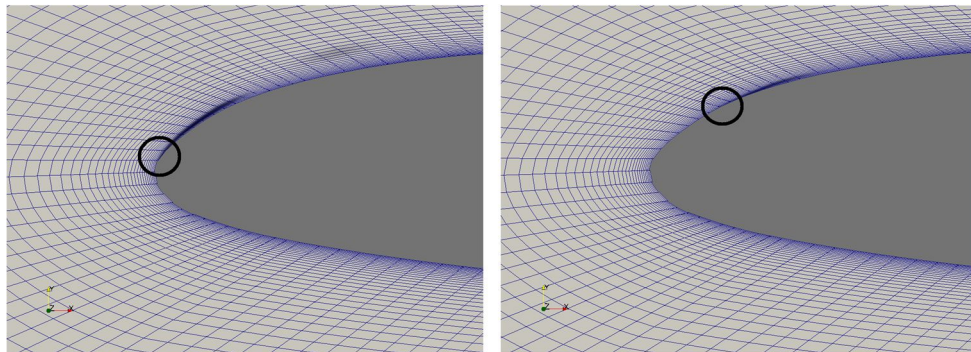


**Figure 4.** The beginning of the cavitation structure for sheet cavitation – left, cloud cavitation – right.

The re-entrant jet starting from trailing edge can be observed for both regimes. It travelled upstream the foil and caused the structures to detach from the foil wall and collapse. For sheet cavitation it was observed that for the whole period the cavitation bubbles are attached to the leading edge, for cloud cavitation the bubbles are separated from leading edge after half of the period, but then the small structure appeared after about 75% of the period. For both regimes the flow near trailing edge was highly unsteady, which was also observed during the experiment.

#### 4.2. Pressure and vapour volume fraction distributions

During the calculations the pressure and vapour volume fraction values were recorded in monitor points located along the foil. In figure 5 the time-averaged (averaged in one period) pressure and vapour volume fraction distributions are shown. For cloud cavitation the pressure on the upper and lower side of the foil was significantly lower, but near the trailing edge, for  $x/c$  coordinate 0.7 to 1, the averaged pressure values were close to each other, which can be caused by the strong unsteady flow. The distribution of the vapour volume fraction shows that for sheet cavitation regime that parameter reached the maximum equal to 0.87 near 18% of  $x/c$  coordinate, which corresponds to the attached bubble cluster near trailing edge. For cloud cavitation the structure was located further from leading edge and the vapour volume fraction was near 0.7 at the same  $x/c$  coordinate. For both cavitation types near the trailing edge the vapour volume fraction increased, which is probably connected to the process of detaching the structures from the foil end.

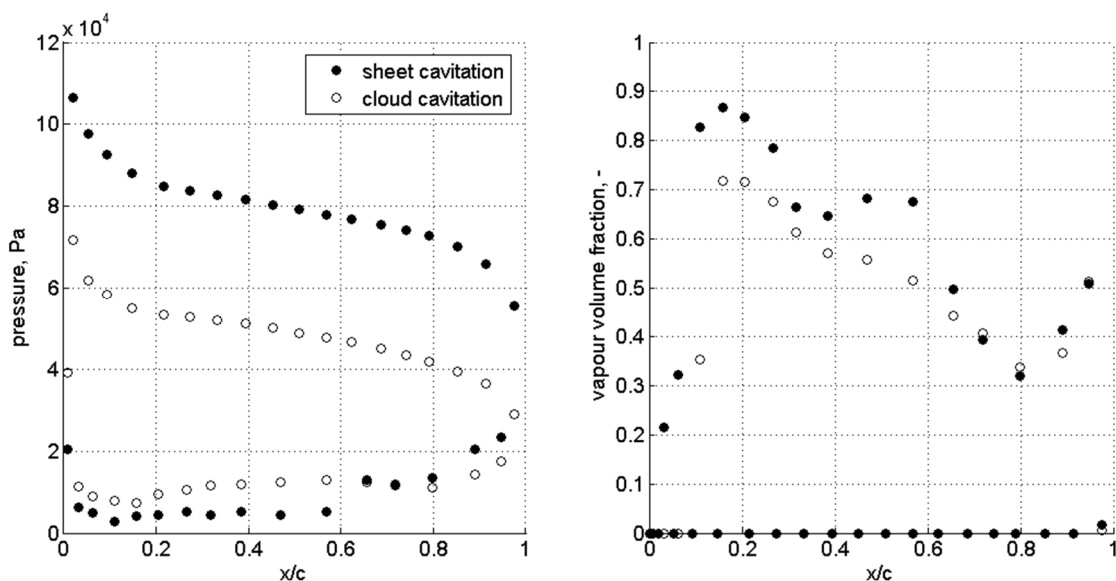


**Figure 5.** Pressure and vapour volume fraction distributions for sheet and cloud cavitation.

### 4.3. Pressure fluctuations

The changes of pressure in time at different monitor points were also studied and are shown in figure 6. The chosen points are located on upper side of the blade, at  $x/c$  coordinate: point 1 – 0, point 2 – 0.2, point 3 – 0.55, point 4 – 0.95.

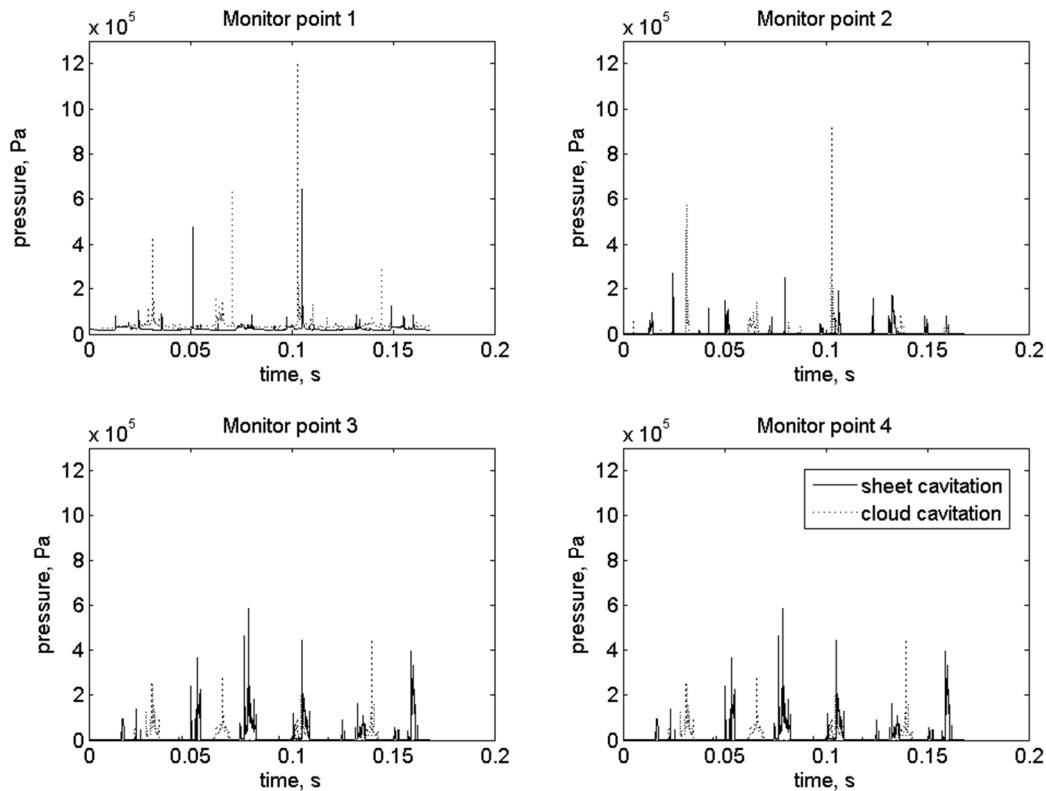


**Figure 6.** Pressure changes in time at monitor points.

For each cavitation regime the peaks of pressure were observed. For cloud cavitation they were much higher, especially for two first monitor points. The pressure changes in these points reached up to  $10^6$  Pa, but the pressure course was in general softer than in case of the other two monitor points. Pressure course in monitor point 4, located closest to the trailing edge, is highly irregular, but without such great peaks of pressure. This confirms the highly unsteady character of cavitation structures near the end of the foil.

The sudden changes of pressure are described in the [1, 2] as one of the characteristic feature of the cavitating flow connected with the process of forming and collapsing of vapour bubbles and need to be further investigated in next numerical simulations.

### 5. Summary

In the paper the results of numerical simulation of two cavitating flow types are presented. The sheet and cloud cavitation regimes were investigated in case of flow over a Clark-Y foil with use of Schnerr & Sauer cavitation model. For both cavitation types the beginning of cavitation structure and the maximum dimensions of cavitation cloud were described and compared to each other. For cloud cavitation the structures were longer and higher, but the beginning of the cavitation cloud was located further from the leading edge of the foil. The shedding frequency for cloud cavitation was in good agreement with the experimental results (30 Hz compared to 20 Hz obtained during the experiment), but for sheet cavitation the frequency of changes was significantly lower comparing to the experimental one (32 Hz in numerical simulation compared to 200 Hz in the experiment). This need to

be solved in the future numerical calculation. The dynamics of parameter changes was generally similar to the one described in the [3] for both regimes. The highly unsteady region near trailing edge as well as re-entrant jet was observed. Also the time-averaged pressure and vapour volume fraction distributions for both cavitation types were compared. The time-averaged vapour volume fraction distributions vary for both regimes, for sheet cavitation the higher values were observed in about 0.2 of normalized chord  $x/c$ , for cloud cavitation they were slightly moved downstream the foil. Near the trailing edge vapour volume fractions increased for both cavitation regimes. The other important aspect was pressure changes in time, as cavitating flow is characterized by great pressure differences occurring in short period of time. During the calculations the pressure was monitored and the sudden peaks of that parameter were observed. The pressure reached up to  $10^6$  Pa. The peaks occurred mainly in the first half of the chord length and they were very rapid. For the second half of the chord, especially for monitor point located near the trailing edge, the changes were not so high but the course of the pressure was strongly irregular.

The results of performed simulations enable to state that the used cavitation model and the chosen OpenFOAM solver capture the dynamics of sheet and cloud cavitation sufficiently. The main features of these flows such as periodic character of changes, forming and collapsing of vapour structures, occurrence of re-entrant jet and sudden pressure fluctuations were observed. However, there are still aspects to improve, such as the obtained shedding frequency, which was far from the experimental data for sheet cavitation regime. That will be the object of interest in the future investigations.

### Acknowledgments

The presented work was supported by the Polish National Science Centre funds within the project UMO-2014/15/B/ST8/00203 and within the project BK/267/RIE5/2015/502.

### References

- [1] Brennen C E 1995 *Cavitation and bubble dynamics* (Oxford: Oxford University Press)
- [2] Franc J P and Michel J M 2004 *Fundamentals of cavitation* (Dordrecht: Kluwer Academic Publishers)
- [3] Wan G, Senocak I, Shyy W, Ikohago T and Cao S 2001 Dynamics of attached turbulent cavitating flows *Progress in Aerospace Sciences* vol 37 pp 551-81
- [4] Puffary B 2006 Numerical modelling of cavitation, design and analysis of high speed pumps *Educational Notes RTO-EN-AVT-143* paper 3, pp 1–54
- [5] Schnerr G H and Sauer J 2001 Physical and numerical modelling of unsteady cavitation dynamics *Fourth International Conference on Multiphase Flow (New Orleans)*
- [6] Gosset A, Diaz Casas V and Lopez Pena F 2010 Evaluation of the CavitatingFoam solver for low Mach number flow around a 2D hydrofoil *Fifth OpenFOAM Workshop (Gothenburg)*
- [7] Wang G, Zhang B, Huang B and Zhang M 2009 Unsteady dynamics of cloud cavitation flows around a hydrofoil *Proceedings of the Seventh International Symposium on Cavitation CAV2009 (Ann Arbor)*
- [8] Roohi E, Zahiri A P and Pasandideh-Fard M 2012 Numerical simulation of cavitation around a two-dimensional hydrofoil using VOF method and LES turbulence *Proceedings of the Eight International Symposium on Cavitation CAV2012*
- [9] Bensow R E and Bark G 2010 Simulating cavitating flows with LES in OpenFOAM *5<sup>th</sup> European Conference On Computational Fluid Dynamics*
- [10] Li Z, Pourquie M and Van Terwisga T 2010 A numerical study of steady and unsteady cavitation on a 2D hydrofoil *Journal of Hydrodynamics* vol 22(5) supplement 770-777
- [11] Li D Q, Grekula M and Lindell P 2009 A modified SST  $k-\omega$  turbulence model to predict the steady and unsteady sheet cavitation on 2D and 3D hydrofoils *Proceedings of the Seventh International Symposium on Cavitation CAV2009 (Ann Arbor)*
- [12] Huang B and Wang G 2011 Partially averaged Navier-Stokes methods for time dependent turbulent cavitating flows *Journal of Hydrodynamics* vol 23(1) pp 26-33